

## Supporting information

# Synthesis and microwave absorbing properties of highly ordered mesoporous crystalline NiFe<sub>2</sub>O<sub>4</sub>

Xin Gu<sup>a,†</sup>, Weimo Zhu<sup>a,†</sup>, Chunjiang Jia<sup>b</sup>, Rui Zhao<sup>c</sup>, Wolfgang Schmidt<sup>b,\*</sup>, Yanqin  
Wang<sup>a,\*</sup>

<sup>a</sup> Key Lab for Advanced Materials, Research Institute of Industrial Catalysis, East  
China University of Science and Technology, Shanghai 200237, P. R. China.

Fax: 86 21 6425 3824; Tel: 86 21 6425; E-mail: wangyanqin@ecust.edu.cn

<sup>b</sup> Max-Planck-Institut für Kohlenforschung, Kaiser-Wilhelm-Platz 1, 45470 Mülheim  
an der Ruhr, Germany. Fax: 49 208 306 2995; Tel: 49 208 306 2370; E-mail:

[schmidt@mpi-muelheim.mpg.de](mailto:schmidt@mpi-muelheim.mpg.de)

<sup>c</sup> Research Branch of Functional Polymer Composites, Institute of Microelectronic  
and Solid State Electronic, University of Electronic Science and Technology of

China, Chengdu 610054, PR China

## ◆ Experiment Part:

**Synthesis of mesoporous nickel/iron spinel:** The chosen synthesis procedure was the “incipient wetness” method. The molar ratio of nickel to iron was fixed to 1:2. Typically, calculated amounts of  $\text{Fe}(\text{NO}_3)_3 \cdot 9\text{H}_2\text{O}$  and  $\text{Ni}(\text{NO}_3)_2 \cdot 6\text{H}_2\text{O}$  were dissolved in de-ionized water. The concentration of the mixture was about  $1.7 \text{ mol L}^{-1}$ . According to the pore volume of the silicate template, 1.1 mL of solution was gradually added to 0.3 g KIT-6 and dried at  $50 \text{ }^\circ\text{C}$  for 3 hours, and calcined at  $200^\circ\text{C}$  for 2 h and at  $750^\circ\text{C}$  for 5h. The impregnation and calcination was repeated twice. 2M NaOH solution was used to dissolve the silica template at  $80 \text{ }^\circ\text{C}$  overnight. The obtained powder was washed with de-ionized water unless the effluent was neutral and then it was dried at  $90 \text{ }^\circ\text{C}$  overnight.

**Characterization:** Powder X-ray diffraction (XRD) patterns were recorded on a Stoe STADI P diffractometer operating in reflection mode with  $\text{Cu K}\alpha$  radiation using a secondary graphite monochromator. Scanning electron microscope (SEM) and energy dispersive X-ray (EDX) analyses were performed on a Hitachi S-3500 N instrument equipped with an Oxford EDX unit (INCA Surveyor Imaging System). Transmission electron microscopy (TEM) was carried out with Hitachi HF 750 instrument. All samples were prepared on lacey carbon films supported by a copper grid.  $\text{N}_2$  sorption measurements were performed with a Micrometrics ASAP 2010 instrument. Magnetic properties of the sample were measured by using a superconducting quantum interference device (SQUID) magnetometer. The mesoporous  $\text{NiFe}_2\text{O}_4$ /paraffin (weight ratio: 1:3) composites were pressed into a toroidal shape with outer diameter of 7 mm and inner diameter of 3 mm for microwave measurements. Complex permittivity and complex permeability were measured with an Agilent Vector Network Analyzer 8720 in the frequency range of 0.5-18 GHz.

◆ **Calculation Part :**

For a single-layer absorbing material backed by a perfect conductor, the input impedance ( $Z_{in}$ ) at the air-material interface is given by

$$Z_{in} = Z_0 \sqrt{\frac{\mu_r}{\epsilon_r}} \tan\left(j \frac{2\pi f d}{c} \sqrt{\mu_r \epsilon_r}\right) \quad (1)$$

Where  $d$  is the thickness of the absorber,  $f$  is the frequency,  $c$  is the velocity of light,  $\mu_r$  is the complex permeability, and  $\epsilon_r$  is the complex permittivity. The reflection loss of a normal incident electromagnetic wave at the absorber surface is given by

$$R = 20 \log \left| \frac{Z_{in} - Z_0}{Z_{in} + Z_0} \right| \quad (2)$$

where  $Z_0$  is the impedance of air.

## Figures

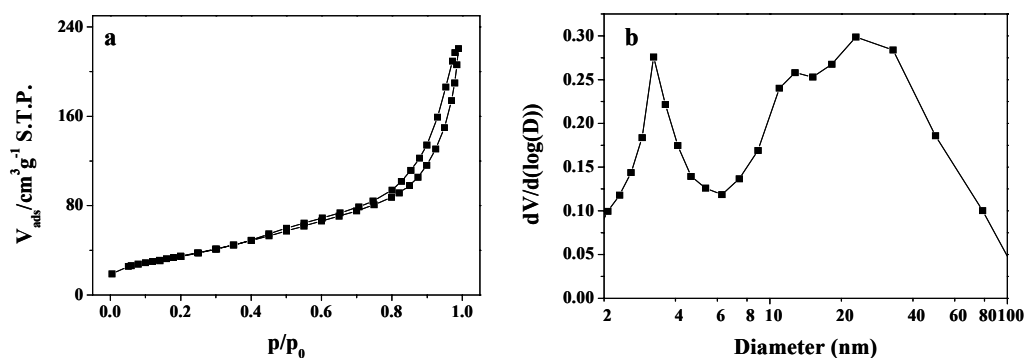


Figure S1. (a) Nitrogen sorption isotherm and (b) BJH pore size distribution of meso- $\text{NiFe}_2\text{O}_4$   
(BJH calculated from the desorption branch).

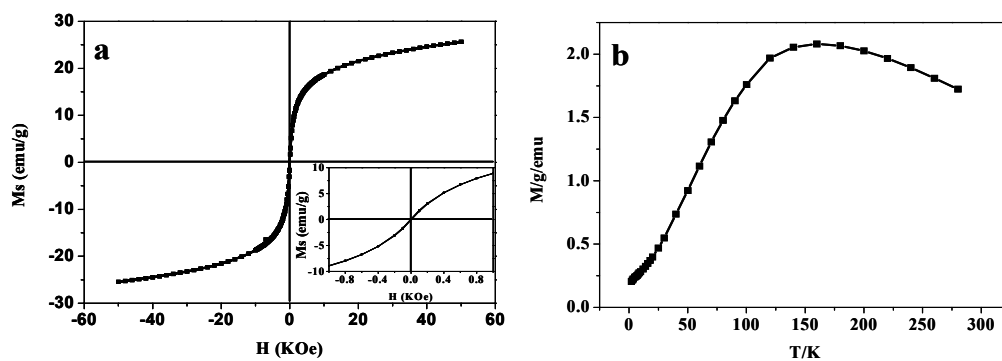


Figure S2. (a) Magnetization curve and zoomed detail (inset) in the low field range and (b) ZFC  
magnetization curve of meso- $\text{NiFe}_2\text{O}_4$ .

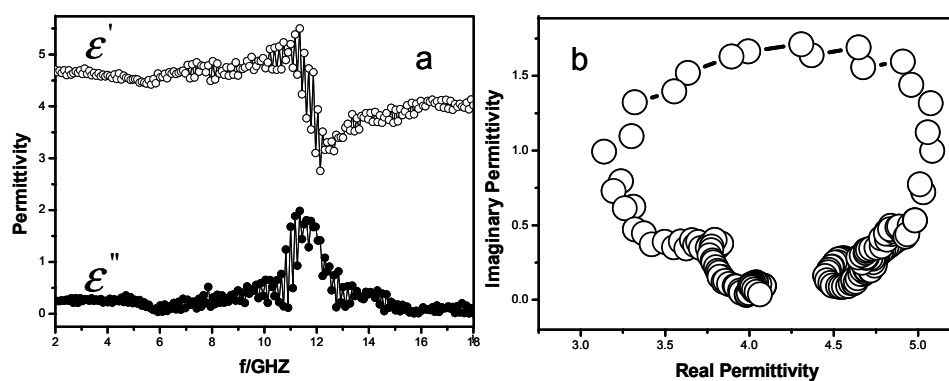
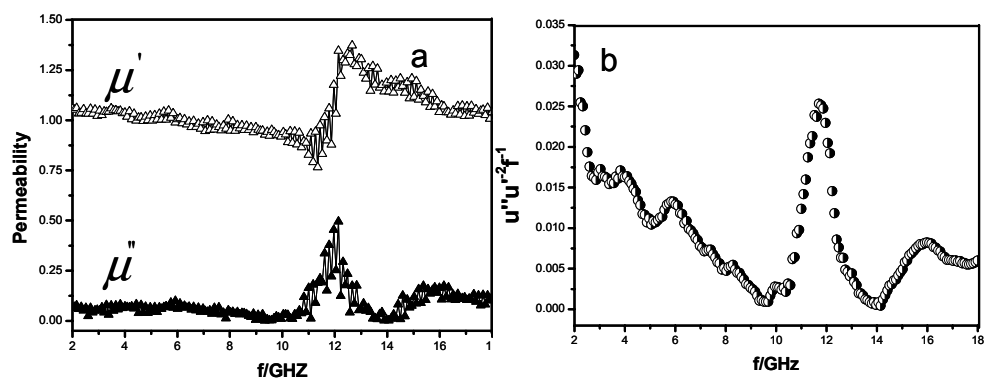


Figure S3. (a) Relative permittivity of mesoporous  $\text{NiFe}_2\text{O}_4$ /paraffin composites as a function of  
frequency and (b) the relation between real part and imaginary part of the complex permittivity  
(Cole-Cole plot).



**Figure S4.** (a) Relative permeability of mesoporous NiFe<sub>2</sub>O<sub>4</sub>/paraffin composites as a function of frequency. (b) The value of  $\mu''(\mu')^{-2}f^{-1}$  as a function of frequency.